ARTICLE

Sustainable Biofuel Production from Brown and Green Macroalgae through the Pyrolysis

Apip Amrullah[1], Widya Fatriasari[2], Novia Amalia Sholeha[3], Edy Hartulistiyoso[4] and Obie Farobie[4,*]

[1]Departement of Mechanical Engineering, Lambung Mangkurat University, Banjarmasin, South Kalimantan, Indonesia

[2]Research Center for Biomass and Bioproducts, National Research and Innovation Agency (BRIN), Cibinong, Bogor, Indonesia

[3]College of Vocational Studies, IPB University, Bogor, West Java, Indonesia

[4]Department of Mechanical and Biosystem Engineering, IPB University, Bogor, West Java, Indonesia

*Corresponding Author: Obie Farobie. Email: obiefarobie@apps.ipb.ac.id

ABSTRACT

The escalating demand for energy coupled with environmental concerns necessitates exploring sustainable alternatives to fossil fuels. The study explores the viability of using large ocean-based seaweeds as a source of third-generation biomass, specifically focusing on their conversion to biofuel via the process of pyrolysis. *Sargassum plagiophyllum* and *Ulva lactuca* represent prevalent forms of macroalgae, posing significant discharge challenges for coastal regions globally. However, the exploration of their potential for bio-oil generation via pyrolysis remains limited. This study investigates the pyrolysis process of *S. plagiophyllum* and *U. lactuca* for biofuel production, aiming to provide valuable insights into their utilization and optimization. Pyrolysis experiments were conducted within temperature ranges of 400°C to 600°C and durations of 10 to 50 min using a batch reactor. The chemical analysis of the synthesized bio-oil indicated it contains critical compounds such as organic acid derivatives, furans, nitrogenous aromatics, and aliphatic hydrocarbons. The effectiveness of converting the initial biomass into bio-oil is significantly influenced by the pace at which the biomass undergoes decomposition, underscoring the importance of comprehending the kinetic aspects of this conversion. By applying the Arrhenius formula, we calculated the activation energies and frequency factors, with the findings for *S. plagiophyllum* being 15.27 kJ/mol and 0.477 s^{-1}, and for *U. lactuca*, the values were 43.17 kJ/mol and 0.351 s^{-1}, correspondingly. These findings underscore the potential of brown and green macroalgae as sustainable sources for biofuel production via pyrolysis, offering insights for further optimization and valorization efforts in the quest for renewable energy solutions.

KEYWORDS

Biomass; bio-oil; macroalgae; pyrolysis; reaction kinetics

1 Introduction

The ever-growing global population and the rapid development of the world have led to unprecedented environmental challenges, particularly in meeting the escalating energy demand. Fossil fuels and petroleum remain the primary sources of energy despite their contribution to atmospheric pollution and depletion of finite resources [1]. However, the overconsumption of petroleum fuels is leading to increased emissions of SO_2, NO_x, and CO_2, resulting in severe environmental problems [2]. Moreover, the continued

consumption of fossil fuels will inevitably deplete petroleum sources worldwide by approximately 2042 without accounting for anticipated increases in consumption [3]. Consequently, the quest for renewable energy substitutes has emerged as a critical priority to address both energy demand and environmental concerns. Biomass emerges as a promising and eco-friendly alternative energy source owing to its wide availability, renewability, and carbon neutrality [4]. Biomass stands as the fourth major source of energy, trailing behind coal, oil, and fossil gas [5]. It is differentiated into four generations, each defined by the origin and use of biomass. Although biochemical methods of biomass transformation are less energy-intensive, their economic viability is hampered due to their exclusive use of cellulose and hemicellulose [6]. In contrast, thermochemical methods like pyrolysis are acknowledged for their higher efficiency and cost-effectiveness in converting biomass into energy [7–9]. Pyrolysis takes place at elevated temperatures, typically between 300°C and 600°C, without the presence of oxygen, producing bio-oil, syngas, and biochar [10–13].

Existing studies have been concentrated on the generation of biofuels from various kinds of biomass, like rice straw, sugarcane bagasse, palm, and corn stover, through the method of pyrolysis, showcasing the versatility of these raw materials for bioenergy [14–16]. However, the reliance on primary biofuel sources might inadvertently lead to a clash between the agricultural markets for food and fuel, potentially driving up prices [17]. While second-generation feedstock does not vie with the production of food, its cultivation still requires essential agricultural inputs such as fertilizer, water, and fertile land. In this context, third-generation biomass, including macroalgae, presents a viable solution. Macroalgae exhibits advantages such as rapid growth, higher biomass yield, shorter harvesting periods, and the ability to grow in different water sources [1]. Among various macroalgae species, *Sargassum plagiophyllum* and *Ulva lactuca* are particularly promising for biofuel production due to their abundance and substantial biomass resources [18]. However, both *S. plagiophyllum* and *U. lactuca* can cause eutrophication issues in aquatic environments [19]. Therefore, the utilization of *S. plagiophyllum* and *U. lactuca* as third-generation biomass holds the promise of offering a viable answer to the challenges that arise from the utilization of first- and second-generation biomass while simultaneously addressing the issue of marine pollution. Nevertheless, the chemical composition of these algae differs. *S. plagiophyllum* contains a higher carbohydrate content than *U. lactuca*, with 53.23% for S. *plagiophyllum* and 40.66% for *U. lactuca*. Conversely, *U. lactuca* contains a higher protein content (22.92%) compared to *S. plagiophyllum* (12.71%) [20]. Hence, a study comparing these macroalgae in terms of their behavior in producing bio-oil would be intriguing.

There has been a limited amount of research examining the biofuel production capabilities of *S. plagiophyllum* and *U. lactuca*. Li et al. [21] conducted rapid pyrolysis experiments within the temperature range of 700°C to 900°C by employing *Sargassum horneri* as a feedstock.

The findings from their study indicated that a significant portion of the liquid by-products from *S. horneri* pyrolysis, reaching the amount of 38.5% of the overall yield, consisted of nitrogen-rich compounds. This composition differed significantly from that of terrestrial plants. Regarding *Ulva* species, limited research has investigated the potential for biofuel production through hydrothermal processes. Amrullah et al. [22] conducted research on the conversion of *U. lactuca* into bio-oil through slow pyrolysis, investigating various temperature ranges (400°C to 600°C) and durations (10 to 50 min). They reported achieving a maximum bio-oil yield of 24.05%, with predominant compounds identified as carboxylic acids ranging from 22.63% to 35.28%. Additionally, Ma et al. [23] explored both non-catalytic and catalytic pyrolysis of *U. prolifera*, observing a bio-oil yield of up to 41.3% using a zeolite catalyst at 400°C. These investigations have contributed to the body of knowledge on converting species such as *Sargassum* sp. and *Ulva* sp. into valuable bio-oil using pyrolysis.

Nevertheless, former research mainly examined the properties of biofuel derived from a single species of macroalgae. Until now, a comparative study between brown and green macroalgae, specifically focusing on pyrolysis for bio-oil production, has not been conducted. This gap limits our understanding of the distinct advantages each type of macroalgae may offer in biofuel applications. Consequently, the purpose of this study is to delve into the production of bio-oil from *S. plagiophyllum* (a representative brown macroalgae) and *U. lactuca* (a representative green macroalgae), marking the first comparative investigation of its kind. The novelty of this work highlights a comprehensive understanding of their properties and explores the pyrolysis degradation pathways and reaction kinetics of both macroalgae, offering detailed insights into the thermal decomposition behavior of these specifically chosen species. Such examination facilitates a deeper understanding of their pyrolytic characteristics and enables optimization of the pyrolysis process for enhanced biofuel production. Overall, this work represents a significant advancement in the exploration of generating bio-oil from *S. plagiophyllum* and *U. lactuca*, as well as elucidating their distinctive attributes and comprehensive decomposition mechanisms.

2 Materials and Methods

2.1 Materials

The marine biomass types, specifically *S. plagiophyllum* and *U. lactuca*, were gathered from the shores of East Lombok Island within the West Nusa Tenggara region of Indonesia. To prepare these macroalgal materials, they were first meticulously cleansed with both tap and distilled water to eliminate any external particles such as sand and oceanic detritus. Subsequent to cleaning, they were subjected to a drying process in an oven at a temperature of 50°C for a duration of three hours. Once thoroughly dried, the materials were pulverized using a device typically employed for grinding coffee beans and then sifted to ensure a size distribution of particle of 60 mesh.

2.2 Analysis of Algal Feedstock

To undertake the basic analysis of the macroalgal biomass, we adhered to the ASTM E1131-08 standards, utilizing a Perkin Elmer Thermogravimetric Analyzer (TGA 4000). The moisture content (MC) was ascertained by heating the feedstock to 110°C under an inert condition and tracking the reduction in mass under a flow of pure nitrogen gas. We measured the volatile matter (VM) content by escalating the temperature of the sample to 900°C and noting the associated mass loss. To determine the ash content (AC), we heated the sample to 900°C for a period of 45 min in an oxidizing atmosphere, and the residual mass was documented. The fixed carbon (FC) percentage was derived through a calculation employing the following formula:

$$FC_{mac} = 100 - [VM_{mac} + MC_{mac} + AC_{mac}] \tag{1}$$

The heating values of the macroalgal feedstock were measured using a Parr 6200 Isoperibol bomb calorimeter in compliance with the ASTM D5865-04 standard procedures. For analyzing the elemental composition, the Leco CHN628 and CHN632 analyzers were employed to assess the levels of carbon, nitrogen, hydrogen, and sulfur. Meanwhile, the oxygen content was calculated by applying the following formula:

$$O\,(\%) = 100 - (C + H + N + S) \tag{2}$$

where, O is oxygen, C is carbon, H is hydrogen, N is nitrogen, and S is sulfur.

The experiment was carried out in triplicate to ensure the accuracy and consistency of the collected data. To present the key outcomes of this investigation, we have tabulated the chemical and elemental analyses of both feedstocks in Table 1.

Table 1: Chemical and elemental analyses of both feedstocks

Feedstock	Chemical analysis (wt%)				Elemental analysis (wt%)					HHV (MJ/kg)
	MC	AC	FC	VM	%C	%H	%N	%S	%O	
U. lactuca	7.18	49.24	1.01	49.75	39.1	6.2	4.46	7.28	42.96	12.04
S. plagiophyllum.	7.02	46.59	3.84	49.57	42.4	5.86	2.72	2.78	46.24	14.46

Note: MC is moisture content, AC is ash content, FC is fixed carbon, VM is volatile matter.

2.3 Pyrolysis Process

The stainless-steel batch vessel was utilized to perform the pyrolysis of both *S. plagiophyllum* and *U. lactuca*, employing a procedure previously outlined and documented in our earlier research [12]. The reactor setup included an electric furnace and a thermocouple for temperature monitoring. The PID controller allowed precise temperature control up to 1000°C. In the pyrolysis procedure, 20 g of desiccated material was introduced into the reactor, followed by the introduction of N_2 gas twice at a rate of 100 mL/min to remove any remaining oxygen. Subsequently, the reactor underwent heating at a flow rate of 20°C/min, starting from room temperatures to reach either 400°C, 500°C, or 600°C, depending on the specific trial. The reactor remained at the designated final temperature for durations of 10, 30, or 50 min. Throughout the operation, vaporous by-products of pyrolysis were condensed and gathered in a liquid sample vial. Following the cooling of the reactor, the resulting biochar was extracted meticulously and weighed. Each trial was conducted twice to ensure precision and reproducibility. The product yields were determined using the subsequent formulas:

$$B_{yield} = \frac{B_{weight}(g)}{Feedstock_{weight}(g)} \times 100 \tag{3}$$

$$BC_{yield} = \frac{BC_{weight}(g)}{Feedstock_{weight}(g)} \times 100 \tag{4}$$

$$G_{yield} = 100 - \left(B_{yield} + BC_{yeild}\right) \tag{5}$$

The symbols "*B*", "*G*", and "*BC*", represent the bio-oil, gas, biochar products, correspondingly.

2.4 Product Analysis

Liquid product (bio-oil) characterization was performed by a GC/MSQP2010 SE system equipped with an Rtx®-5MS capillary column (Shimadzu, Japan). Previous studies have extensively analyzed bio-oil [20]. Before being introduced into the GC/MS system, the liquid product underwent a decantation process to separate the organic phase from the aqueous layer. Following this, the organic phase was diluted with dichloromethane at a volumetric ratio of 1 to 4. Subsequently, 1 μL of the resulting solution was utilized for injection into the GC/MS instrument. The analysis was performed with a column flow rate set at 2 mL/min and a split ratio maintained at 10:1. Helium served as the carrier gas for this process. The thermal gradient initiated at a temperature of 40°C, held steady for one minute before increasing by 10°C every minute up to 150°C, where it was sustained for five minutes. Subsequently, the temperature was elevated to 300°C at the same rate and held constant for thirty minutes. The mass spectrometer's ion source operated with an electron ionization (EI) energy of 70 eV, and the detector was regulated at a temperature of 250°C. The molecular fragments deriving from the bio-oil vapors were analyzed over a mass-to-charge (m/z) spectrum spanning from 35 to 700 Da. The comparison of mass spectra was conducted by utilizing the NIST2008 c2.0 dataset to ascertain the constituents of bio-oil. The solid products were oven-dried and measured using an electronic scale.

2.5 Kinetic Model

The reaction rate in the pyrolysis process is a key factor in the thermal decomposition of solid biomass. Comprehending the dynamics of solid biomass conversion necessitates a comprehensive examination of the reaction rate parameters. Fig. 1 presents a model that illustrates the degradation process of macroalgae during slow pyrolysis. This model offers valuable insights into the pyrolysis process and the transformation of solid biomass.
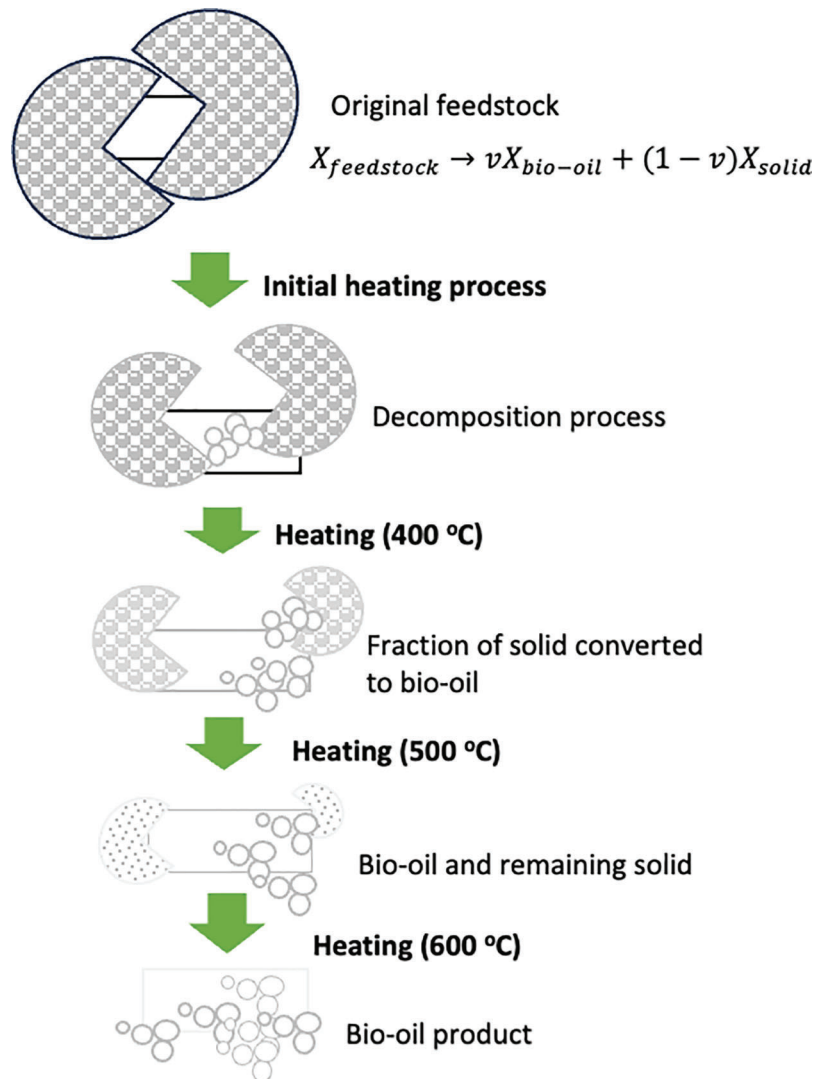

Original feedstock
$$X_{feedstock} \rightarrow vX_{bio-oil} + (1-v)X_{solid}$$

Initial heating process

Decomposition process

Heating (400 °C)

Fraction of solid converted to bio-oil

Heating (500 °C)

Bio-oil and remaining solid

Heating (600 °C)

Bio-oil product

Figure 1: An illustration of solids degradation during the slow pyrolysis of macroalgae

By adopting the assumption that the solid material decomposition adheres to first-order kinetics, it is feasible to quantify both the proportion and rate constant linked with the degradation process. Hence, the mathematical model can be expressed as follows:

$$X_{feedstock} \rightarrow vX_{bio-oil} + (1-v)X_{solid} \tag{6}$$

In this context, $X_{feedstock}$ denotes the proportion of the original macroalgae feedstock. The variable v signifies the portion of the solid that is converted into bio-oil. Meanwhile, $X_{bio\text{-}oil}$ and X_{solid} indicate the proportions of bio-oil and the leftover solid, respectively.

Assuming a first-order reaction, the rate equation for the feedstock at time t can be established based on the following formula:

$$\frac{d\left[X_{feedstock}\right]}{dt} = -k\left[X_{feedstock}\right] \tag{7}$$

where, $X_{feedstock}$ denotes the concentration of feedstock fraction.

Taking into account the concept of mass balance, the balance equation can be articulated as follows:

$$\begin{aligned}
&\left[X_{feedstock}\right] + \left[X_{bio-oil}\right] + \left[X_{solid}\right] = \text{constant} \\
&= \left[X_{feedstock}\right]_t + \left[X_{bio-oil}\right]_t + \left[X_{solid}\right]_t = \left[X_{feedstock}\right]_t
\end{aligned} \tag{8}$$

where, the notation i and t signify the initial state and the total quantity of feedstock throughout the pyrolysis process. Concurrently, the concentration of $\left[X_{feedstock}\right]$ can be formulated as:

$$\left[X_{feedstock}\right] = \frac{1-v}{v}\left[X_{bio-oil}\right] \tag{9}$$

By replacing Eq. (9) with Eq. (8), one can articulate the mass balance as:

$$\begin{aligned}
\left[X_{feedstock}\right] &= \left[X_{feedstock}\right]_t - \left[X_{bio-oil}\right] - \left[X_{solid}\right] \\
&= \left[X_{feedstock}\right]_t - \left[X_{bio-oil}\right] - \frac{1-v}{v}\left[X_{bio-oil}\right] \\
&= \left[X_{feedstock}\right]_t - \left(1 + \frac{1-v}{v}\right)\left[X_{bio-oil}\right] \\
&= \left[X_{feedstock}\right]_t - \frac{1}{v}\left[X_{bio-oil}\right]
\end{aligned} \tag{10}$$

Subsequently, by inserting Eq. (10) into Eq. (7), the rate of change can be identified as:

$$\frac{d}{dt}\left(\left[X_{feedstock}\right]_t - \frac{1}{v}\left[X_{bio-oil}\right]\right) = -k\left(\left[X_{feedstock}\right]_t - \frac{1}{v}\left[X_{bio-oil}\right]\right) \tag{11}$$

Eq. (11) can be reformulated as:

$$\frac{d}{dt}\left(X_{bio-oil}\right) = vk\left(\left[X_{feedstock}\right]_t - \frac{1}{v}\left[X_{bio-oil}\right]\right) \tag{12}$$

At the same time, the yield of bio-oil can be expressed as:

$$Y_{bio-oil} = \frac{\left[X_{bio-oil}\right]}{\left[X_{feedstock}\right]_t} \tag{13}$$

Therefore, Eq. (12) can be calculated as:

$$\frac{d}{dt}Y_{bio-oil} = vk - kY_{bio-oil} \tag{14}$$

Eq. (14) can be simplified to the following form:

$$\frac{dY_{bio-oil}}{vk - kY_{bio-oil}} = dt \tag{15}$$

$$ln(v - Y_{bio-oil}) = -kt + C \tag{16}$$

$$Y_{bio-oil} = v - A\exp(-kt) \tag{17}$$

At $t = 0$, the yield of bio-oil is $Y_{bio-oil,i}$:

$$Y_{bio-oil} = v - (v - Y_{bio-oil,i})\,exp(-kt) \tag{18}$$

The rate constant can be calculated using the Arrhenius equation in the following manner:

$$k\exp\left(-\frac{E_a}{RT}\right) \tag{19}$$

Here, T stands for temperature, A denotes the pre-exponential factor, E_a is the activation energy, and R signifies the gas constant.

Ultimately, upon substituting the Arrhenius equation into Eq. (18), the equation can be expressed as:

$$Y_{bio-oil} = v - (v - Y_{bio-oil,i})\,exp\left(-A\,exp\left(-\frac{E_a}{RT}\right)t\right) \tag{20}$$

3 Results and Discussion

3.1 Influence of Temperature and Reaction Time on the Product Fraction

To investigate how temperature affects the distribution of products during the pyrolysis of *S. plagiophyllum* and *U. lactuca*, we conducted pyrolysis at temperatures varying between 400°C and 600°C. A marginal decline in biochar production was noted with the escalation of pyrolysis temperature from 400°C to 600°C for both *S. plagiophyllum* and *U. lactuca* (Fig. 2). It is noted that the pyrolysis was conducted with a fixed holding time of 50 min. This trend suggests that at elevated temperatures, there is a more pronounced degradation of macroalgal feedstock, likely contributing to this outcome.
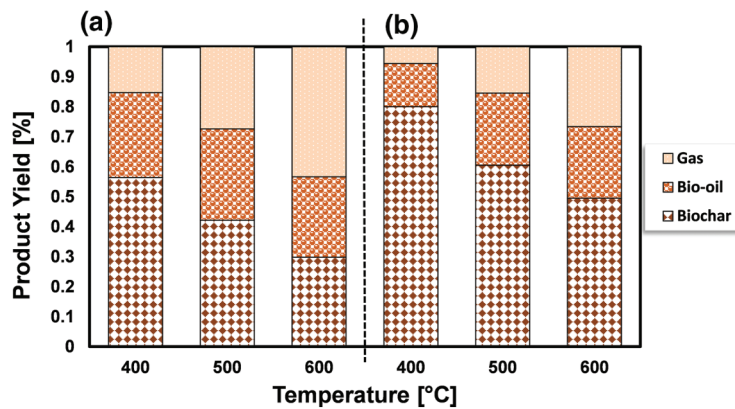

Figure 2: The impact of temperature on the distribution of products for the pyrolysis of (a) *S. plagiophyllum* and (b) *U. lactuca*

Notably, the generation of liquid products escalated with the temperature elevation from 400°C to 500°C; nevertheless, it diminished as the temperature further rose to 600°C. The upsurge in bio-oil production between pyrolysis temperatures of 400°C and 500°C might be ascribed to heightened initial degradation mechanisms of algal feedstock, encompassing thermal cracking and dehydration. Conversely, an earlier investigation pointed out a reduction in bio-oil yield as the temperature hit 600°C [24]. This decline could be due to amplified cracking of substances at temperatures surpassing 500°C, leading to the formation of non-condensable gases like CH_4, CO, and CO_2. The substantial augmentation in gas production substantiates this finding as the temperature climbed from 400°C to 600°C. The observed rise in gas production could be attributed to increased levels of groups I and II elements in macroalgae, as evidenced in prior research by Farobie et al. [20]. Temperature, however, is not the sole determinant influencing the pyrolysis process; other factors, such as reaction time, also wield significant influence. Fig. 3 presents the results of product distribution for reaction durations of 10–50 min.
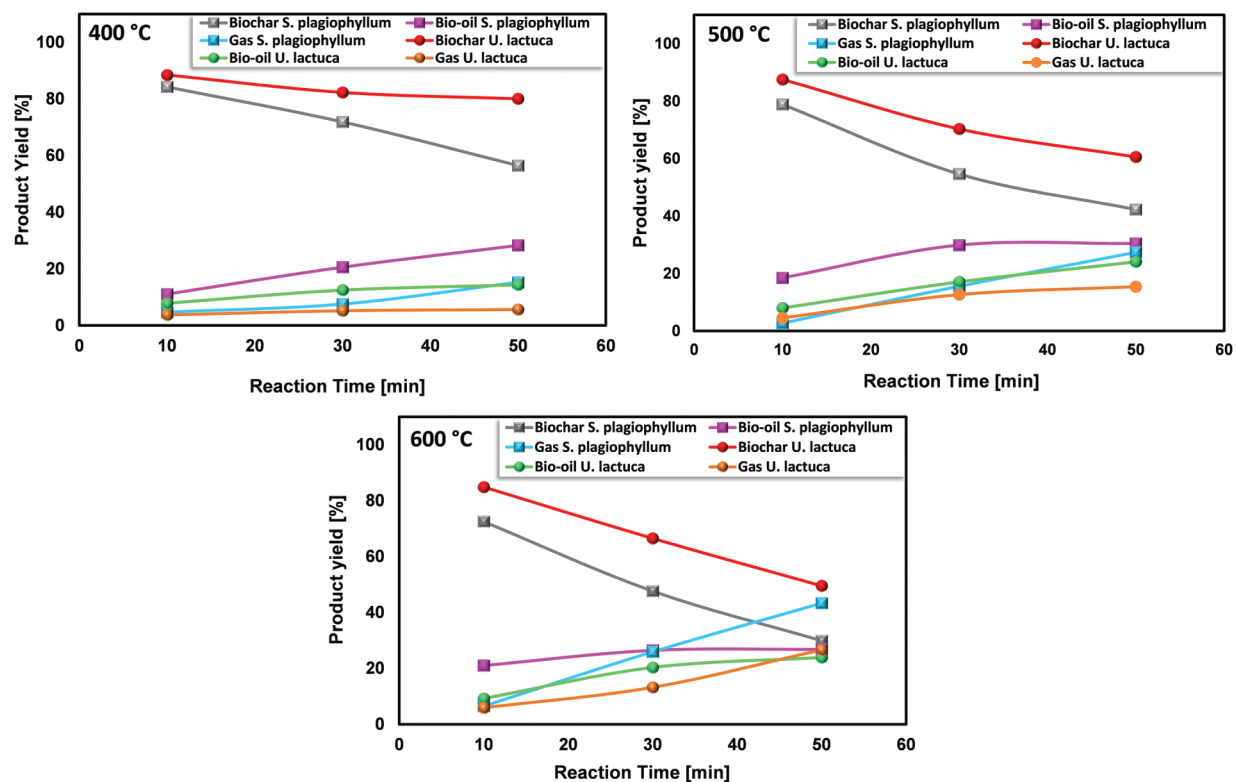

Figure 3: The impact of time on the product distributions of *S. plagiophyllum* and *U. lactuca* pyrolysis (reaction time 10, 30, and 50 min)

At 400°C, there was a noticeable yet not significant rise in bio-oil generation. The incompleteness of the pyrolysis process of *S. plagiophyllum* becomes apparent as the bio-oil yield amounted to only 11.05% following a 10-min retention period. In comparison, the yield of bio-oil from the pyrolysis of *U. lactuca* was relatively lower at 7.82%, possibly because *Ulva*'s structure is more delicate and less susceptible to proper destruction at 400°C. Additionally, biochar yields decreased significantly with longer retention times, indicating considerable decomposition of macroalgal feedstock results from the breaking down of dense hydrocarbons over prolonged reaction durations. This finding is in line with an earlier investigation

conducted by Choi et al. [25], wherein it was noted that extending the retention time for the pyrolysis of *Saccharina japonica* enhanced bio-oil production while decreasing biochar production.

The transformation efficiency of algal biomass into bio-oil demonstrates a considerable increase at 500°C in comparison to 400°C, which varies depending on the biomass type. For *S. plagiophyllum*, the bio-oil yields were 18.5%, 29.9%, and 30.4%, following retention times of 10, 30, and 50 min, correspondingly. In contrast, *U. lactuca* displayed yields of bio-oil as high as 7.98%, 12.49%, and 24.05% after identical reaction durations. However, elevating the temperature to 600°C did not significantly enhance bio-oil production, even with extended reaction times of 30 to 50 min. In general, elevating the temperature from 400°C to 600°C resulted in reduced biochar production and a higher generation of gaseous by-products, which can be ascribed to the breakdown of volatile vapors. This observation aligns with some previous studies. For instance, Aboulkas et al. [26] explored the influence of temperature on the distribution of pyrolysis products from algal waste pyrolysis, noting a reduction in biochar production from 52.09 to 40.36 wt% as the temperature rose from 400°C to 600°C.

In this study, we found that slow pyrolysis leads to more biochar than bio-oil when we use it on certain types of seaweed, like *S. plagiophyllum* and *U. lactuca*. We chose slow pyrolysis specifically to closely examine how these seaweeds break down with heat. This detailed look is important for figuring out how to make more biofuel from seaweed in the future. The relatively low bio-oil yield, as observed, indeed presents a challenge. However, it opens new chances to improve and try different methods like fast pyrolysis, alongside a rigorous optimization of process conditions. Such optimization efforts could include adjustments in temperature, reaction time, and the preparation of seaweed biomass. Each of these factors can significantly influence the pyrolysis outcome and, consequently, the balance between biochar and bio-oil production. This study starts off by finding better ways to turn seaweed into biofuel.

3.2 Effect of Temperature on Properties of Bio-Oil

Bio-oil obtained from the pyrolysis of *S. plagiophyllum* and *U. lactuca* exhibited diverse chemical compounds. Predominantly, the bio-oil from both *S. plagiophyllum* and *U. lactuca* pyrolysis comprised aliphatic hydrocarbons, organic acids, N-hydrocyclic substances, amides, phenolics, and ketones. The percentage of peak area for specific compounds was compared to explore variations across different pyrolysis temperatures. This analysis focused on major chemicals with an area percentage greater than 0.5%. Fig. 4 illustrates the compositional differences observed under varied temperatures and macroalgal species. It is noteworthy that the pyrolysis was conducted with a holding time of 50 min. Bio-oils from *S. plagiophyllum* and *U. lactuca* mostly contained furan derivatives, carboxylic acids, N-hydrocyclic substances, and phenolics.
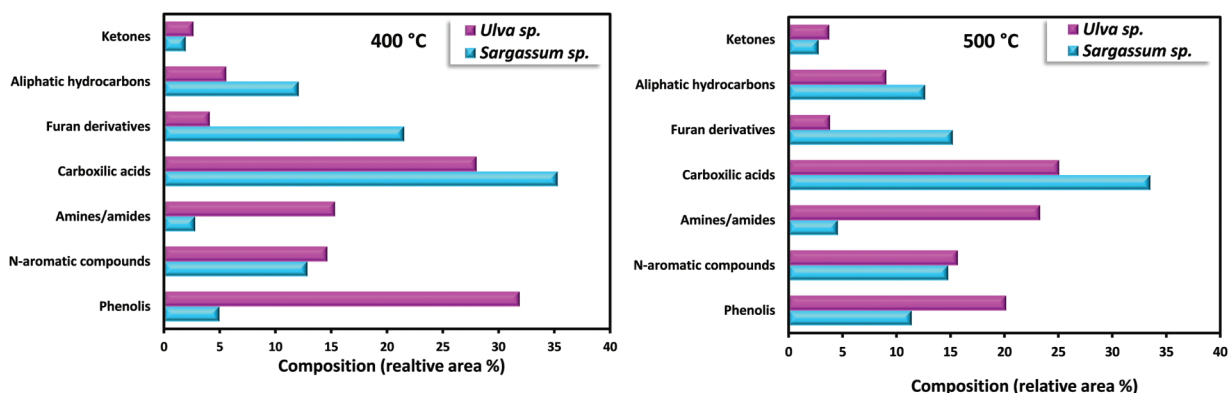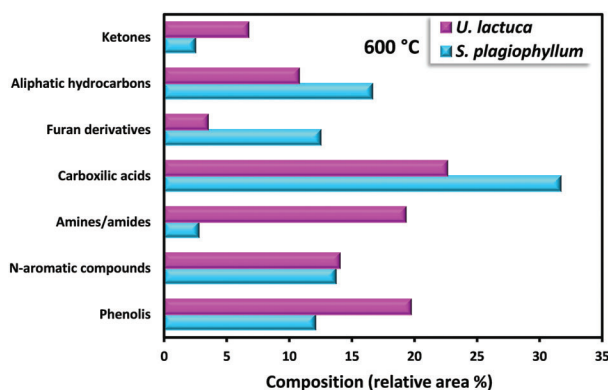

Figure 4: (Continued)

Figure 4: Detection of distinct substances in the produced bio-oil during the pyrolysis of *S. plagiophyllum* and *U. lactuca*

The primary compound identified is carboxylic acid, constituting approximately 31.68%–35.28% of *S. plagiophyllum*, whereas *U. lactuca* contains a lower proportion of carboxylic acid, ranging from 22.6% to 28.02%. The generation of short-chain organic acids is associated with lipid degradation mechanisms. These results are in good agreement with a prior investigation by Iaccarino et al. [24], which highlighted carboxylic acids as the primary constituents in bio-oil derived from *Salicornia bigelovii* pyrolysis. Interestingly, the general pattern of carboxylic acid prevalence in bio-oil declines with rising pyrolysis temperatures for both *S. plagiophyllum* and *U. lactuca*. Specifically, the percentages are as follows: 35.01%; 28.02% (at 400°C) > 33.51%; 25.07% (at 500°C) > 31.68%; 22.62% (at 600°C), respectively. This trend is attributed to temperature-induced cracking and organic acid decarboxylation, leading to short-chain aliphatic hydrocarbons forming during pyrolysis. Consequently, the prevalence of aliphatic hydrocarbons increases with rising pyrolysis temperature.

Bio-oil production from *S. plagiophyllum* involves the generation of various furan derivatives through pyrolysis, such as 5-hydroxymethylfurfural (5-HMF). The conventional approach to acquiring furan derivatives entails the pyrolysis of polysaccharides and glucose-based carbohydrates from seaweed. In our study, we noted a decline in the preference for furan derivatives in liquid fraction as the temperature decreased, as demonstrated by the following sequence: 21.53% > 15.21% > 12.51% for the temperatures of 400°C, 500°C, and 600°C, correspondingly. This pattern contrasts sharply with observations from different *U. lactuca*. The furan area in *U. lactuca* is relatively small, showing the following trend: 4.09% (400°C) > 3.82% (500°C) > 3.52 (600°C), which may be attributed to the distinct structure of *Ulva* species. Another pathway for furan production involves a coordinated reaction of electrocyclic from fragmentation of cellulose, known as Grob fragmentation, succeeded by cyclization and dehydration mechanisms, as reported by Gautam et al. [27]. Additionally, Zhou et al. [28] highlighted that furan derivatives can be obtained through various dehydration steps and ring-opening xylose reactions. It is noteworthy that the pyrolysis of *S. plagiophyllum* and *U. lactuca* yielded a greater proportion of N-hydrocylic substances (12.86%–14.78%; 14.64%–15.67%) compared to the pyrolysis of other land-based biomass [29]. This discrepancy could be ascribed to the greater protein content found in macroalgae compared to land-based lignin-derived biomass [1]. The generation of N-heterocyclic derivatives often occurs through the cyclization processes of amino acids resulting from the decomposition of proteins at higher temperatures. Additionally, N-heterocyclic derivatives can also be formed through the decomposition of the Maillard reaction, which is the reaction between carbohydrates and amino acids [30]. This finding corroborates earlier research by Iaccarino et al. [24], where amino acids were demonstrated to

go through dehydration, decarboxylation, and cyclization processes, resulting in the generation of N-heterocyclic derivatives during *Salicornia bigelovii* pyrolysis.

The quantity of phenolic substances presents in bio-oil generated from *S. plagiophyllum* is notably lower than that from *U. lactuca*. In *S. plagiophyllum*, the selectivity of phenolic compounds ranged from 4.96% to 12.10%, while in *U. lactuca*, it varied between 19.73% and 31.88% at 400°C to 600°C, respectively. It has been previously suggested that aromatic compounds' steam reaction could lead to the generation of phenols. Moreover, the breakdown of side chains in phenolic compounds may be induced by elevated temperatures, resulting in hydrocarbon production [31]. This phenomenon contrasts with terrestrial lignocellulosic biomass pyrolysis, which yields significant amounts of phenolic chemicals (ranging from 28.19% to 65.56%) [32]. One plausible explanation for this difference is the lower lignin content found in macroalgae compared to terrestrial plant biomass [26]. According to Iaccarino et al. [24], phenolic compounds can form as moisture interacts with aromatic compounds. Additionally, macroalgae contain various phytochemical metabolites that contribute to phenolic compound formation. The pyrolysis of *S. plagiophyllum* and *U. lactuca* revealed the presence of significant amine/amide compounds. The relative area of amine/amide compounds in *S. plagiophyllum* appeared to be much smaller (2.7%–4.6%) compared to *U. lactuca*, which ranged between 15.33% and 23.31% across temperatures of 400°C–600°C. This variation might be linked to the protein composition of macroalgae, with the compounds likely originating from the degradation and decarboxylation of amino acids.

Aliphatic hydrocarbons were detected in the bio-oil extracted from *S. plagiophyllum* and *U. lactuca*, likely resulting from the decarboxylation reaction following the breakdown of long-chain organic acids. Additionally, cracking, ring-opening, and dehydration of cellulose could contribute to the formation of hydrocarbons. The preference for aliphatic hydrocarbons gradually rose with temperature for both raw materials, as evidenced by the following trend: 12.08%; 5.58% (400°C) < 12.65%; 9.05% (500°C) < 16.65%; 10.79% (600°C) for *S. plagiophyllum* and *U. lactuca*, respectively. Furthermore, during the pyrolysis of polysaccharides, i.e., hemicellulose and cellulose, both types of macroalgae contained trace levels of ketone derivatives, ranging from 1.94% to 2.77% for *S. plagiophyllum* and 2.64% to 6.75% for *U. lactuca*.

3.3 Effect of Temperature on Solid Degradation

To evaluate the solid degradation behavior, we conducted thermogravimetric analysis on *S. plagiophyllum* and *U. lactuca* and their respective biochar. By assessing the thermal stability of the biochar, TGA provides valuable insights into its thermal behavior, which is essential for understanding its potential applications, including its use as a soil enhancer, in carbon sequestration, or as a feedstock in the production of activated carbon. Fig. 5 illustrates the thermogravimetric analysis results performed on *S. plagiophyllum* and *U. lactuca* and their associated biochar.

Thermogravimetric analysis was conducted to determine the mass loss of *S. plagiophyllum* and *U. lactuca* during the pyrolysis process, as well as their respective biochars. The mass loss of *S. plagiophyllum* occurred at temperatures of 278°C and 438°C, with a percentage of 15.4% and 56.4%, respectively. This indicates that devolatilization is the primary cause of mass loss during pyrolysis. In comparison, *U. lactuca* displayed a lower mass loss at temperatures ranging from 310°C to 554°C, with a loss of 17%–20% at 310°C and 42% at 554°C. According to Kim et al. [31], the reduction in biomass mass reflects the decomposition of large molecules like carbohydrates and proteins. Furthermore, it was noted that significant mass reduction of *S. plagiophyllum* and *U. lactuca* occurred at temperatures above 600°C, with a loss of approximately 68.1% and 50.2%, respectively. One possible explanation for this phenomenon is macroalgae's degradation of inorganic substances, particularly metal polysaccharides [11].
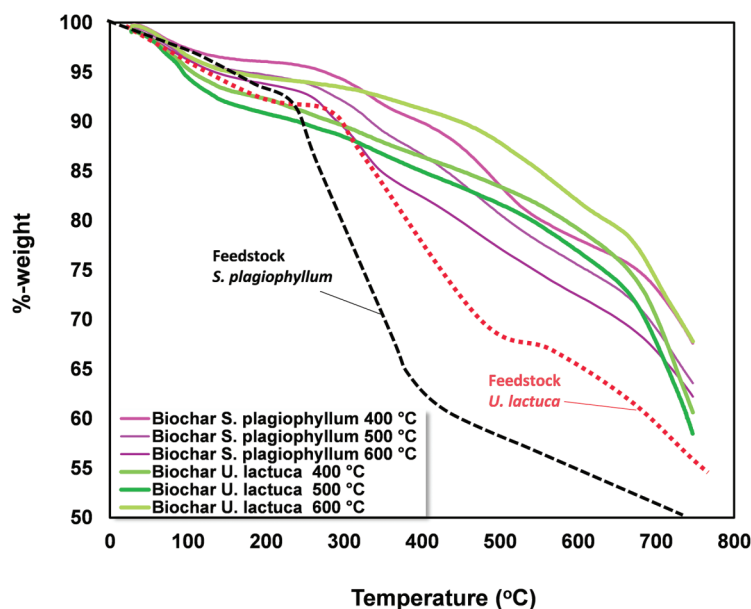
Figure 5: Thermogravimetric analysis of *S. plagiophyllum*, *U. lactuca*, and biochar

Notably, half of the mass of *S. plagiophyllum* was decomposed at temperatures above 398°C, while for *U. lactuca*, it occurred at temperatures above 428°C. Therefore, the pyrolysis of *S. plagiophyllum* and *U. lactuca* should be carried out at higher temperatures than 398°C. As for biochar, no substantial mass reduction was noted, even at temperatures as low as 300°C, with only around 10.1% mass loss identified at 400°C. This can be attributed to the fact that biochar primarily consists of polyaromatic chemicals, which exhibit greater resilience to decomposition compared to proteins and carbohydrates. However, when the temperature was increased to 600°C, a mass loss of approximately 21.9% was found in the biochar. This can be ascribed to the production of gaseous substances through thermal decomposition at higher temperatures [20].

3.4 Reaction Kinetics of Solid Degradation

The least-square error (LSE) technique was utilized to ascertain the reaction rate and quantify the conversion of solids into liquids. By utilizing Eq. (20) above, the model-predicted data can be calculated. The experimental data was corrected using the estimated correlation value between temperature and bio-oil production for the two macroalgae varieties, *S. plagiophyllum* and *U. lactuca*. Fig. 6 showcases the results of this correction, demonstrating a favorable alignment between the experimental and predicted data. This strong agreement between the two sets of data indicates the effectiveness of the LSE method in accurately estimating the relationship between temperature and bio-oil production.

Fig. 6a presents the results of the curve fitting analysis, depicting the comparison between the experimental value and the predicted model representing the relationship between temperature and the yield of bio-oil. The finding from the experiment showed excellent agreement with the estimated values, further supported by the high R^2 value of 0.9982, as validated by the parity plots. The Arrhenius plots (Fig. 6b) illustrate the thermal decomposition of *S. plagiophyllum* and *U. lactuca*. As predicted, a direct linear relationship was observed between the reciprocal of temperature (1/T) and ln k. This observation suggests that the array of pyrolysis products deriving from macroalgae conforms to the Arrhenius equation.
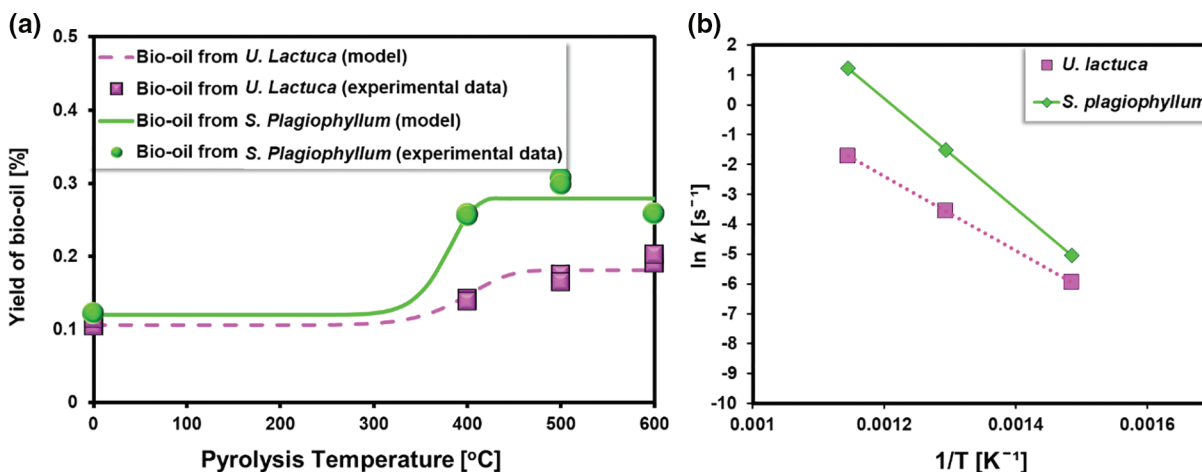
Figure 6: (a) Curve fitting for bio-oil yield and (b) Arrhenius plots (Exp condition: Feedstock: *S. plagiophyllum* and *U. lactuca*, Temperature range 400°C–600°C)

In the case of the pyrolysis of *S. plagiophyllum*, it was found that the pre-exponential factor had an approximate value of 0.477 s^{-1}, while for *U. lactuca*, the estimated value was around 0.351 s^{-1}. Additionally, it was determined that the activation energy for the pyrolysis of the two raw materials was found to be 15.27 and 43.17 kJ mol^{-1}, respectively. These values were notably lower than those of previous studies involving terrestrial biomass, such as coconut and almond shells. Amrullah et al. [33] found that the activation energy for coconut shell pyrolysis was approximately 153 kJ mol^{-1}, while Genieva et al. [34] determined an activation energy for almond shell pyrolysis was about 125.3 kJ mol^{-1}. The disparities can be ascribed to variations in the chemical composition of biomass. Macroalgae contains predominantly carbohydrates and possesses lower amounts of lignin compared to land-lignocellulosic biomass, resulting in a lower energy requirement for its decomposition.

4 Conclusion

This study delved into the behavior of *S. plagiophyllum* and *U. lactuca* raw materials through slow pyrolysis, aiming to gain insights into their potential valorization. The pyrolysis reactions occurred between 400°C and 600°C over a reaction duration spanning 10 to 50 min, impacting the distribution and properties of the resultant bio-oil. Increasing the temperature and extending the reaction time led to higher bio-oil and gas production while suppressing the yield of biochar. This phenomenon may stem from the heightened degradation of macroalgae at elevated temperatures or the continued degradation of biochar. The pyrolysis process of *S. plagiophyllum* and *U. lactuca* yielded bio-oil, comprising a composition of carboxylic acids (25.07%–35.01%; 22.6%–28.02%), furan derivatives (12.51%–21.53%; 3.54%–4.09%), aliphatic hydrocarbons (12.08%–16.65%; 5.58%–10.79%), and N-heterocyclic derivatives (12.86%–14.78%; 14.64%–15.67%), respectively. By employing a kinetic model, the degradation rate of *S. plagiophyllum* and *U. lactuca* in the pyrolysis process was estimated, and the experimental values showed a strong agreement with the kinetic model. The pyrolysis facilitated the release of macroalgal cells, resulting in a higher yield of bio-oil. The decomposition of both *S. plagiophyllum* and *U. lactuca* adhered to Arrhenius' rule. The activation energy for *S. plagiophyllum* was determined at 15.27 kJ mol^{-1} with a rate constant of 0.477 s^{-1}, while for *U. lactuca*, it was identified at 43.17 kJ mol^{-1} with a rate constant of 0.351 s^{-1}. Future research endeavors should explore downstream process integration to enhance further the utilization of *S. plagiophyllum* and *U. lactuca* for bioenergy and high-value chemical production. This study lays a foundational understanding for leveraging macroalgae as a sustainable

feedstock for bioenergy generation, contributing to advancing renewable energy solutions and environmental sustainability initiatives.

Author Contributions: Writing-orignal draft, O.F. and A.A.; conceptualization, O.F.; methodology, O.F., W.F., A.A., E.H. and N.A.S.; investigation, A.A. and W.F.; formal analysis, A.A. and W.F.; resources, O.F.; data curation, O.F., W.F, A.A., E.H. and N.A.S.; writing-review and editing, O.F., W.F., A.A., E.H. and N.A.S.; supervision, O.F. and E.H.; project administration, O.F. All authors have read and agreed to the published version of the manuscript.

Availability of Data and Materials: Data will be made available on request.

Conflicts of Interest: The authors declare that they have no conflicts of interest to report regarding the present study.

References

1. Farobie O, Matsumura Y, Syaftika N, Amrullah A, Hartulistiyoso E, Bayu A, et al. Recent advancement on hydrogen production from macroalgae via supercritical water gasification. Bioresour Technol Rep. 2021;16:100844. doi:10.1016/j.biteb.2021.100844.

2. Bond JQ, Upadhye AA, Olcay H, Tompsett GA, Jae J, Xing R, et al. Production of renewable jet fuel range alkanes and commodity chemicals from integrated catalytic processing of biomass. Energy Environ Sci. 2014;7(4):1500–23. doi:10.1039/c3ee43846e.

3. Dhanavath KN, Bankupalli S, Sugali CS, Perupogu V, Nandury SV, Bhargava S, et al. Optimization of process parameters for slow pyrolysis of neem press seed cake for liquid and char production. J Environ Chem Eng. 2019;7(1):102905. doi:10.1016/j.jece.2019.102905.

4. Destek MA, Sarkodie SA, Asamoah EF. Does biomass energy drive environmental sustainability? An SDG perspective for top five biomass consuming countries. Biomass Bioenergy. 2021;149:106076. doi:10.1016/j.biombioe.2021.106076.

5. Li CY, Wu JY, Dai YJ, Wang CH. Multi-criteria optimization of a biomass gasification-based combined cooling, heating, and power system integrated with an organic Rankine cycle in different climate zones in China. Energy Convers Manag. 2021;243. doi:10.1016/j.enconman.2021.114364.

6. Yang H, Liu Y, Bai G, Zhang Y, Xia S. Study on the co-pyrolysis characteristics of oil-based drill cuttings and lees. Biomass Bioenergy. 2022;160:106436. doi:10.1016/j.biombioe.2022.106436.

7. Santoso A, Sholikhah A, Sumari S. Effect of Active zeolite in the pyrolysis of polypropylene and low density polyethylene types of plastic waste. J Renew Mater. 2022;10(11):2781–9. doi:10.32604/jrm.2022.021401.

8. Xu L, Xie G, Zhou X. Catalytic pyrolysis of soybean oil with CaO/Bio-Char based catalyst to produce high quality biofuel. J Renew Mater. 2022;10(12):3107–18. doi:10.32604/jrm.2022.020691.

9. Dhyani V, Bhaskar T. A comprehensive review on the pyrolysis of lignocellulosic biomass. Renew Energy. 2018;129:695–716. doi:10.1016/j.renene.2017.04.035.

10. Liu Y, Song Y, Ran C, Siyal AA, Jiang Z, Chtaeva P, et al. Characterization and analysis of condensates and non-condensable gases from furfural residue via fast pyrolysis in a bubbling fluidized bed reactor. Waste Manag. 2021;125:77–86. doi:10.1016/j.wasman.2021.02.025.

11. Wu P, Zhang X, Wang J, Yang J, Peng X, Feng L, et al. Pyrolysis of aquatic fern and macroalgae biomass into bio-oil: comparison and optimization of operational parameters using response surface methodology. J Energy Inst. 2021;97:194–202. doi:10.1016/j.joei.2021.04.010.

12. Amrullah A, Farobie O, Widyanto R. Pyrolysis of purun tikus (*Eleocharis dulcis*): product distributions and reaction kinetics. Bioresour Technol Rep. 2021;13:100642. doi:10.1016/j.biteb.2021.100642.

13. Wang J, Zhang B, Cheng H, Xu Z. Enhancing hydrocarbon-rich bio-oil production via catalytic pyrolysis fortified with microorganism pretreatment. J Renew Mater. 2023;11(10):3595–612. doi:10.32604/jrm.2023.030005.

14. Luo Z, Wang S, Liao Y, Zhou J, Gu Y, Cen K. Research on biomass fast pyrolysis for liquid fuel. Biomass Bioenergy. 2004;26(5):455–62. doi:10.1016/j.biombioe.2003.04.001.

15. Ly HV, Kim J, Kim SS. Pyrolysis characteristics and kinetics of palm fiber in a closed reactor. Renew Energy. 2013;54:91–5. doi:10.1016/j.renene.2012.08.053.

16. Hu E, Tian Y, Yang Y, Dai C, Li M, Li C, et al. Pyrolysis behaviors of corn stover in new two-stage rotary kiln with baffle. J Anal Appl Pyrolysis. 2022;161:105398. doi:10.1016/j.jaap.2021.105398.

17. Rulli MC, Bellomi D, Cazzoli A, Carolis GD, D'Odorico P. The water-land-food nexus of first-generation biofuels. Sci Rep. 2016;6:1–10. doi:10.1038/srep22521.

18. Davis D, Simister R, Campbell S, Marston M, Bose S, McQueen-Mason J, et al. Biomass composition of the golden tide pelagic seaweeds *Sargassum fluitans* and *S. natans* (morphotypes I and VIII) to inform valorisation pathways. Sci Total Environ. 2021;762:143134. doi:10.1016/j.scitotenv.2020.143134.

19. Human LRD, Adams JB, Allanson BR. Insights into the cause of an Ulva lactuca Linnaeus bloom in the Knysna Estuary. South African J Bot. 2016;107:55–62. doi:10.1016/j.sajb.2016.05.016.

20. Farobie O, Amrullah A, Bayu A, Syaftika N, Anis LA, Hartulistiyoso E. In-depth study of bio-oil and biochar production from macroalgae *Sargassum* sp. *via* slow pyrolysis. RSC Adv. 2022;12(16):9567–78. doi:10.1039/d2ra00702a.

21. Li J, Zhu Y, Wang C, Wei W, Liu Z, Tian Y, et al. Golden seaweed tides from beach inundations as a valuable sustainable fuel resource: fast pyrolysis characteristics, product distribution and pathway study on *Sargassum horneri* based on model compounds. Algal Res. 2020;48:101888. doi:10.1016/j.algal.2020.101888.

22. Amrullah A, Farobie O, Bayu A, Syaftika N, Hartulistiyoso E, Moheimani NR, et al. Slow pyrolysis of *Ulva lactuca* (Chlorophyta) for sustainable production of bio-oil and biochar. Sustainability. 2022;14(6):1–14. doi:10.3390/su14063233.

23. Ma C, Geng J, Zhang D, Ning X. Non-catalytic and catalytic pyrolysis of Ulva prolifera macroalgae for production of quality bio-oil. J Energy Inst. 2020;93(1):303–11. doi:10.1016/j.joei.2019.03.001.

24. Iaccarino A, Gautam R, Sarathy SM. Bio-oil and biochar production from halophyte biomass: effects of pre-treatment and temperature on Salicornia bigelovii pyrolysis. Sustain Energy Fuels. 2021;5(8):2234–48. doi:10.1039/d0se01664k.

25. Choi JH, Kim SS, Suh DJ, Jang EJ, Min KI, Woo HC. Characterization of the bio-oil and bio-char produced by fixed bed pyrolysis of the brown alga *Saccharina japonica*. Korean J Chem Eng. 2016;33(9):2691–8. doi:10.1007/s11814-016-0131-5.

26. Aboulkas A, Hammani H, El Achaby M, Bilal E, Barakat A, El harfi K. Valorization of algal waste via pyrolysis in a fixed-bed reactor: production and characterization of bio-oil and bio-char. Bioresour Technol. 2017;243:400–8. doi:10.1016/j.biortech.2017.06.098.

27. Gautam R, Shyam S, Reddy BR, Govindaraju K, Vinu R. Microwave-assisted pyrolysis and analytical fast pyrolysis of macroalgae: product analysis and effect of heating mechanism. Sustain Energy Fuels. 2019;3(11):3009–20. doi:10.1039/c9se00162j.

28. Zhou S, Liang H, Han L, Huang G, Yang Z. The influence of manure feedstock, slow pyrolysis, and hydrothermal temperature on manure thermochemical and combustion properties. Waste Manag. 2019;88:85–95. doi:10.1016/j.wasman.2019.03.025.

29. Persson H, Yang W. Catalytic pyrolysis of demineralized lignocellulosic biomass. Fuel. 2019;252:200–9. doi:10.1016/j.fuel.2019.04.087.

30. Wang Y, Wang S, Leng F, Chen J, Zhu L, Luo Z. Separation and characterization of pyrolytic lignins from the heavy fraction of bio-oil by molecular distillation. Sep Purif Technol. 2015;152:123–32. doi:10.1016/j.seppur.2015.08.011.

31. Kim JY, Moon J, Lee JH, Jin X, Choi JW. Conversion of phenol intermediates into aromatic hydrocarbons over various zeolites during lignin pyrolysis. Fuel. 2020;279:118484. doi:10.1016/j.fuel.2020.118484.

32. Su Y, Liu L, Zhang S, Xu D, Du H, Cheng Y. A green route for pyrolysis poly-generation of typical high ash biomass, rice husk: effects on simultaneous production of carbonic oxide-rich syngas, phenol-abundant bio-oil, high-adsorption porous carbon and amorphous silicon dioxide. Bioresour Technol. 2020;295:122243. doi:10.1016/j.biortech.2019.122243.

33. Amrullah A, Farobie O, Pramono GP. Solid degradation and its kinetics on phenol-rich bio-oil production from pyrolysis of coconut shell and Lamtoro wood residue. Korean J Chem Eng. 2022;39(2):389–97. doi:10.1007/s11814-021-0923-0.

34. Genieva S, Gonsalvesh L, Georgieva V, Tavlieva M, Vlaev L. Kinetic analysis and pyrolysis mechanism of raw and impregnated almond shells. Thermochim Acta. 2021;698:178877. doi:10.1016/j.tca.2021.178877.